

A GENERAL PRELIMINARY SIZING PROCEDURE FOR PURE-ELECTRIC AND HYBRID-ELECTRIC AIRPLANES

Lorenzo Trainelli, Carlo E. D. Riboldi, Francesco Salucci, Alberto Rolando

*Department of Aerospace Science and Technology, Politecnico di Milano,
Via G. La Masa 34, 20156 Milano, Italy. Email: lorenzo.trainelli@polimi.it*

KEYWORDS: aircraft sizing, conceptual design, hybrid-electric powertrain, sustainable aviation

ABSTRACT:

A general procedure for the preliminary sizing of innovative pure-electric and hybrid-electric airplanes is presented, with the ambition to provide a tool applicable to propeller-driven, fixed-wing vehicles of arbitrary size and mission requirements.

1. INTRODUCTION

Pure-electric (PE) and hybrid-electric (HE) manned aircraft are currently attracting much attention in view of near-future applications, aiming to improved sustainability in aviation, as well as to renew short-haul air travel for enhanced personal mobility. As a consequence, a growing number of concepts and applications is undergoing advanced development.

The present contribution introduces a general procedure for the preliminary sizing of pure-electric (PE) and hybrid-electric (HE), with the ambition to provide a tool applicable to propeller-driven, fixed-wing vehicles of arbitrary size and mission requirements. This fills up a need that is keenly felt nowadays. In fact, when looking at the blossoming literature about electric aircraft, the typical situation is either that of a retrofit of an existing airframe, or of design considerations more or less specific to a single application.

The present approach to the determination of the design weights, the sizing of powertrain components, and the global dimensions of the aircraft, is pursued by an integrated performance evaluation procedure, with specific provisions for electrically-driven aircraft and even for conventionally-powered ones. Hybrid-electric powertrains and their onboard integration are of primary interest in the prototypal developments of the H2020 MAHEPA project (Modular Approach to Hybrid Electric Propulsion Architecture, www.mahepa.eu) [1], which shall soon provide measured laboratory and flight test data to make HYPERION further accurate and reliable, as well as in the preliminary design activities within the Clean Sky UNIFIER19 project (Community Friendly Miniliner, www.unifier19.eu).

Power and energy mission requirements lead to the sizing of electric motors and batteries, as well as the power generation system (PGS) and its fuel system. Other specifications peculiar to electrically-driven aircraft, such as PE-mode operations below a given altitude or energy recuperation through propeller wind-milling during descent, are considered, providing predictions related to future realistic operational uses.

2. FORMULATION

2.1. General

The following discusses a methodology that generates optimal PE and HE sizing solutions to specified mission, technology, certification and other applicable requirements. Optimality involves minimum design mass (Maximum Take-off Mass, MTOM), as well as selected energy and power management strategies during the sizing mission. Off-design performance analysis can be carried out, once a design solution has been defined, allowing for extensive parametric studies.

The methodology combines the ability to resort to historical-statistical estimations and direct modelling of aircraft main subsystems, in a modular fashion. Aiming at maximum generality, in view of extended conceptual studies, trade-off assessments, and sensitivity analyses, propulsive architectures currently implemented include conventional (thermal), pure-electric, and serial hybrid-electric powertrains. The electric option may include batteries and/or hydrogen fuel cells, while the hybrid-electric options may use different types of fuel-burning engines. In addition, electrically-driven thrust generation may be based on a combination of massive motors and distributed motors (Distributed Electric Propulsion, DEP), for which a basic aero-propulsive interaction model is provided.

2.2. Mass breakdown, power, and wing surface

The starting point for PE and HE sizing-oriented modelling is a more articulated mass breakdown formulation compared to that traditionally used in the preliminary sizing of conventionally-powered aircraft. This is necessary, as the classical separation – at least at conceptual level – between design mass estimation and power and wing

loadings cannot hold with PE and HE aircraft [2–4]. In fact, point performance and mission profile requirements are inherently coupled when it comes to the sizing of the energy sources and power supply devices. This departs from the classical approach, where power needs determine the engine sizing, while mission energy is separately taken into account by the fuel fraction method [5,6].

The proposed approach applies to the preliminary sizing of PE and serial HE propeller-driven aircraft, where the former can be seen as a special case of the latter, where the PGS is absent.

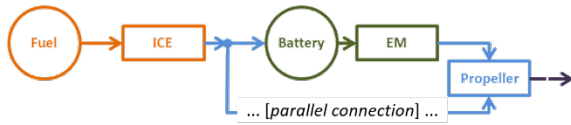


Figure 1. Serial hybrid-electric architecture.

Fig. 1 depicts the conceptual scheme of the serial propulsive architecture, which implies the presence of an electric motor (EM) driving each propeller, powered by a battery pack (BP) and a PGS for electric power supply [7]. The latter is typically represented by a hydrocarbon-burning internal combustion engine (ICE), being either a reciprocating engine or a turboshaft, coupled with an electric generator. Other possibilities for the PGS include the case of a fuel cell system, as discussed in [8]. In the present context, a PE aircraft is obtained as the case of a serial HE one without a PGS.

The sizing procedure is based on the breakdown of the design gross mass, i.e. the maximum take-off mass (MTOM) M_{mto} , cast as

$$M_{mto} = M_p + M_a + M_m + M_b + M_g + M_f \quad (1)$$

where M_p represents payload mass, M_a non-propulsive airframe mass, M_m electric motor mass, M_b BP mass, M_g PGS mass, and M_f fuel mass. Non-propulsive airframe mass is a term introduced here that takes into account of all airframe masses except those related to the powertrain. The traditional approach for conventionally-powered airplanes is based on the simpler breakdown $M_{mto} = M_p + M_{oe} + M_f$, where M_{oe} represents operational empty mass. This is typically estimated through historical statistical regressions based on similar existing aircraft, a process that is not applicable for PE and HE aircraft, due to the lack of consolidated data for these new airplane types.

In the present case, the sum ($M_a + M_m + M_b + M_g$) corresponds to the operational empty mass, but its estimation must be achieved term by term, by appropriate usage of historical statistical regressions at subsystem level, or other applicable models, such as physics-based analytic ones. Models of either kind pertaining to EMs, BP, and

PGS involve their power output characteristics, making the process of weight sizing inherently coupled with power and wing surface estimation, contrary than in conventionally-powered aircraft. In addition, energy storage characteristics enter the sizing of BP and fuel tank.

Therefore, all power and energy mission requirements must be considered in order to solve Eq. 1 simultaneously with the choice of an appropriate design point on the Sizing Matrix Plot (SMP, also known as performance matching plot [5,6]). This consists in the determination of the design power loading W_{mto}/P_s and wing loading W_{mto}/S , being $W_{mto} = M_{mto}g$ the design gross weight, P_s the shaft brake-power and S the wing surface, which guarantees a number of point and terminal (take-off and landing) performance requirements derived from mission analysis, certification standards, and other design specifications.

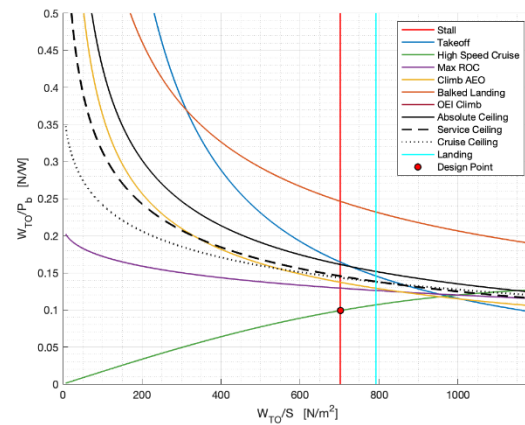


Figure 2. Sizing matrix plot for a commuter aircraft under CS23 regulations.

Fig. 2 shows a typical SMP for a CS23 aircraft. Each curve in the diagram corresponds to a given performance requirement, ranging from flight characteristics to field performance. The former include stalling speed in the landing configuration (blue line), maximum rate of climb in all-engine-operative (AEO) condition (yellow line), maximum rate of climb in one-engine-inoperative (OEI) condition at continuous power (purple line) and peak power (green line) settings, maximum cruising speed (cyan line). The latter include maximum take-off distance (red line), landing distance (not shown, as it lies on the right of the stalling speed boundary), and bailed landing (brown line) requirements. As the curves represent feasibility boundaries, admissible values for the design power loading/wing loading pair lie under and on the left of each curve, and the admissible area is found as the region which satisfies all performance constraints. In the case of Fig. 2, the feasibility region is bounded, from increasing values of the design

wing loading, by the cruising speed, then maximum OEI rate of climb at peak power, and eventually by the landing stalling speed. Any point in this region may be chosen for the design solution. However, a typical choice is to stay close to the corner where the vertical line of the stalling speed crosses the nearest constraint curve, yielding an aircraft with minimum wing size at given design gross weight.

2.3. Batteries and electric motors

Batteries are considered through their specific energy (ratio of stored energy on mass) e_b and specific power (ratio of output power on mass) p_b . These parameters are characteristic of a given battery cell technology and are further modified to provide for the inefficiencies related to cell stacking into packs. The mass of the battery pack M_b is then obtained as the larger between $M_b^E = E_b e_b$ and $M_b^P = P_b p_b$, where E_b is the energy to be provided by the BP according to the mission needs and P_b is its maximum power output.

The latter, for PE and serial-HE aircraft corresponds to maximum power conditions, i.e. take-off and initial climb. Indeed, in both cases, it is the EM fed by the BP that drives the propeller, so the entirety of the motive power comes from the batteries. In the serial-HE case, this is necessary, in order to allow flying terminal manoeuvres and, more generally, trajectories below a given “hybrid transition altitude”, in PE mode, i.e. with the PGS shut off.

This is a crucial advantage granted by the serial architecture (in contrast to the parallel one, where a mechanical mixing of motive power from both EMs and ICEs occurs), allowing zero-emission and a considerable degree of noise abatement in the vicinity of airports [9]. Therefore, the BP is sized to fulfil maximum mission power first (sizing to power), and then increased, if needed, to provide energy for the flight phases below the hybrid transition altitude (sizing to energy).

Upper and lower threshold values of the BP state of charge (SOC) different from full charge and null charge are considered, motivated by the need to preserve battery capacity and health upon a number of discharging/recharging cycles. Also, BP charge/discharge rates can be considered, on the same grounds.

Electric motors are considered mainly through their specific power p_m , so that $M_m = P_s p_m$. This parameter is retrieved from a historical statistical regression [2,3]. Among other important parameters in the sizing lies the motor's extra power capability, i.e. the possibility to draw substantially higher power values for limited period of time, which may cover take-off and initial climb requirements, lowering the rated power reference value, and consequently the EM mass.

2.4. Power generation system and fuel

The PGS combines an ICE (either reciprocating or turboshaft) and an electric generator, to provide electric energy for the BP and EM needs. Its sizing relies on its overall specific power p_g , so that $M_g = P_g p_g$, where P_g is a parameter that can be selected by the designer. This power sizing is based on the extra power obtained with respect to power required for cruising: a basic condition is to size the PGS so that it sustains cruise with no contribution by the BP, while a wider flexibility is obtained when more power is delivered by the PGS, allowing for BP recharge in flight.

The fuel quantity for the design sizing mission is clearly related to the energy delivered through the PGS according to the various phases of the mission profile (including adequate reserves). Fuel energy density e_f (ratio of stored chemical energy on mass) is the primary parameter used in the sizing, $M_f = E_f e_f$.

2.5. Non-propulsive airframe mass

The operational empty mass fraction M_{oe}/M_{mto} is a typical datum retrieved by historical statistical regressions for conventionally-powered aircraft [5,6]. The M_{oe} term comprises the crew, the load-bearing structure, on-board systems unrelated to the powertrain, including the landing gear, and the engines with their ancillary systems. In order to derive a suitable estimation of the non-propulsive airframe mass M_a for preliminary sizing purposes, a dedicated procedure has been deployed based on empty mass and engine mass and power data, allowing to deprive empty mass data of the share pertaining to engines. The latter are retrieved using a historical statistical regression, based on their specific power. Upon validation of this approach, with regard to existing aircraft spanning multiple weight categories, the difference between operational empty mass and engine mass is assumed as the quantity of interest, i.e. $M_a = M_{oe} - M_e$, where M_e represents the mass of the engines in conventionally-powered airplanes.

2.6. Mission profile

Power and energy requirements to be applied in the mass estimation are obtained through the analysis of the sizing mission profile. When considering a typical transfer mission for a civil passenger or freight airplane, the profile is composed by take-off, climb, cruise at constant altitude, descent, loiter at constant altitude (according to applicable regulations), approach, and landing. A diversion to an alternate destination can be considered as well. Apart from terminal ones, all phases are typically flown at constant calibrated airspeed (CAS).

Specific requirements apply to each phase in relation to power and energy management. First, flight below the hybrid transition altitude must be operated in PE mode, including take-off, initial climb, final descent, landing, and possibly loiter as well. Also, energy recuperation in gliding flight by deriving battery recharging power from wind-milling propeller(s) can be considered.

Above the hybrid transition altitude, the PGS can be switched on according to various programs, relative to diverse options for in-flight energy management. These may be inspired by various alternative criteria (such as minimizing the number of battery discharge/recharge cycles per flight, or minimizing the fuel burned per flight) and are clearly allowed by the possibility to draw power for flight from two independent power sources, i.e. the BP and PGS. A study illustrating the differences in the sizing of the aircraft, and consequently in the fuel consumption for a given sizing mission, when different energy management strategies are applied has been discussed in [4].

Finally, minimum values for BP SOC and fuel remaining at mission completion can be specified, to provide for emergency manoeuvres and other contingencies, including a diversion, as required by applicable aeronautical regulations.

3. IMPLEMENTATION

The methodology consists in a two-step procedure. First, the requirements from mission analysis are imposed together with certification standards, and other design specifications, a first-guess design point is chosen on the SMP, and an iterative calculation gathering all elements discussed above is carried out for the weight sizing until Eq. 1 converges. This provides an initial solution in terms of mass breakdown, power sizing and wing sizing, together with the estimation of some basic quantities of geometric and aerodynamic nature (such as the wing aspect ratio and the aircraft drag polar curve).

The initial solution is used to start another iterative computation in which the full sizing mission is simulated by a time-marching algorithm. This procedure allows to take into account the time evolution of the dynamics of the powertrain in a finer manner, typically leading to adjustments on the initial estimations.

This process was implemented in a computational tool named Hyperion (HYbrid PERFORMANCE Simulation). Its schematics is depicted in Fig. 3, where "AircraftSizing" stands for the core of the operations leading to the initial solution, while "FMS" (Flight Mission Simulation) represents the time-marching computation block.

The process starts by solving Eq. 1 through an initial MTOM guess and looping until convergence, while accommodating all mission requirements and performance specifications derived by the applicable certification basis or other design

considerations and bringing into play a number of parameters yielded by the market analysis and technology survey that are normally carried out prior to the start of conceptual design.

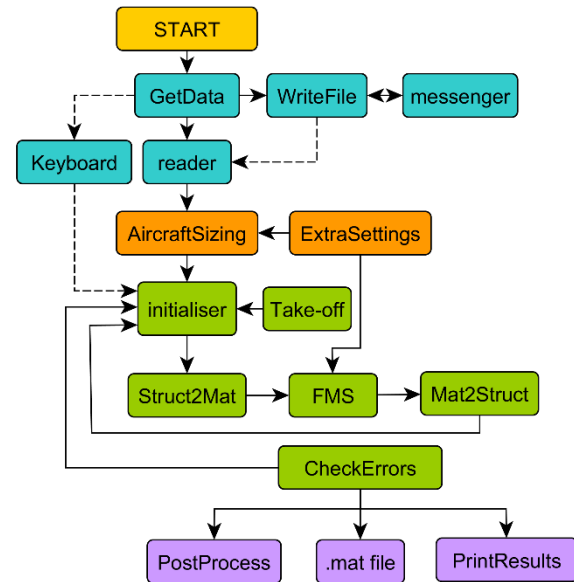


Figure 3. Flowchart of the Hyperion preliminary sizing tool.

Within "AircraftSizing", all components of Eq. 1 are adjusted in a fully coupled manner, taking into account changes in power and energy needs arising from changes in mass of the various components, and viceversa, and seeking minimum gross design weight. Once convergence is achieved, the time simulation in "FMS" is deployed, and the masses of energy storage components, i.e. BP and fuel tank, are corrected in order to satisfy mission requirements punctually. This typically leads to small adjustments that do not require adaption of the masses of the other variable components, i.e. EMs, PGS, and non-propulsive airframe. In case adjustments are more substantial, the process can be repeated feeding "AircraftSizing" with the "FMS" solution as the initial guess.

4. VALIDATION

The proposed methodology has been subjected to an extensive validation effort, with the aim of checking its ability in supporting design exercises across the wider possible aircraft categories.

As hybrid-electric aircraft are not yet diffused and the few examples are mainly prototypal and do not represent a statistically meaningful population, a first task involved the comparison of results obtained for conventionally-powered aircraft with available data. To do so, a number of existing airplanes certified under both CS23 and CS25 have been considered, ranging from General Aviation to large regional turboprops. In the

following, three examples are reported. In addition, to provide a validation concerning a HE aircraft, a case study has been carried out by taking reference on the Pipistrel Panthera Hybrid, one of the two prototypes currently being developed in the MAHEPA project.

4.1. Microfeeder

The first case study involves a small commuter aircraft, the P2012 Traveller, a 11-seat airplane designed and manufactured by the Italian Tecnam. It is a piston-engined, high-wing aircraft powered by a pair of Lycoming TEO540C1As, providing for a maximum cruising speed of 190 kn. This aircraft represents a typical candidate for the roles of “microfeeder” and “miniliner”. These terms identify small liners intended to operate from a diffuse network of small airports and even airstrips in order to feed passengers to and fro regularly scheduled flights at major airports (microfeeder) or to commute passengers between small airports (miniliner). The microfeeder concept, recently explored in [10,11], is of primary concern in the research carried out in the MAHEPA project, as a possible key component in the future development of a more connected transportation network based on a novel class of environmentally-friendly, short-haul airliners [12,13].

The Hyperion design solution was obtained by imposing a sizing mission characterized by the official data for this type, including a range of 1,750 km with 9 passengers on board.

Table 1. Validation for the Tecnam P2012 microfeeder aircraft.

| Tecnam P2012 | M_{mto} [kg] | M_a [kg] | M_f [kg] | S [m ²] | P_b [kW] |
|--------------|----------------|------------|------------|-----------------------|------------|
| Real | 3,600 | 2,250 | 275 | 25.4 | 560 |
| Simulated | 3,327 | 1,927 | 304 | 24.0 | 443 |
| Error [%] | -7.6 | -14.4 | +10.5 | -5.5 | -20.9 |

Tab. 1 shows some of the results obtained for this case: “Real” stands for official data, “Simulated” by the Hyperion results, and “Error” for the percentage difference, i.e. the latter minus the former, divided by the former. As seen, the difference in MTOM amounts to less than 8%, with the Hyperion solution being the lighter. This is the effect of the larger error found in the non-propulsive airframe mass, amounting to nearly 15%. Indeed, by considering a population of similar aircraft, the operational empty mass of the P2012 looks somewhat higher than “average”, and this is not seized by the proposed procedure, as it relies on historical statistical regressions for the sizing of airframe and engine masses. The lighter overall weight induces a lower need for installed power, with a 21% difference, which in turn implies a lower weight for the engines. The wing surface is smaller by 5%.

Although these results are not perfectly matching,

in view of the significant scattering encountered in the lower end of the CS23 commuter category, especially with respect to the operational empty mass fraction M_{oe}/M_{mto} , this case can be considered sufficient for a preliminary validation. In fact, running Hyperion in a “constrained mode”, by imposing the operational empty mass at the actual value instead than estimating it through a regression, provides highly closer results.

4.2. Commuter

The second case study involves a larger aircraft, the nineteen-passenger Beechcraft 1900D, which lies at the upper end of the CS23 commuter category. It is a 19-passenger, pressurized, turboprop, low-wing aircraft powered by a pair of Pratt & Whitney Canada PT6A, providing for a cruising speed of 280 kn. Aircraft in the same class, often employed as regional liners, also represent possible candidates for the roles of microfeeder and miniliner. In particular, a 19-passenger aircraft is the target of the preliminary design activities in project UNIFIER19.

The Hyperion design solution was obtained by imposing a sizing mission characterized by the official data for this type, including a range of 700 km with 19 passengers on board.

Table 2. Validation for the Beechcraft 1900D commuter aircraft.

| Beech 1900D | M_{mto} [kg] | M_a [kg] | M_f [kg] | S [m ²] | P_b [kW] |
|-------------|----------------|------------|------------|-----------------------|------------|
| Real | 7,764 | 4,732 | 894 | 28.8 | 1,910 |
| Simulated | 7,659 | 4,707 | 814 | 28.2 | 1,860 |
| Error [%] | -1.4 | -0.5 | -8.9 | -2.1 | -2.6 |

Tab. 2 shows some of the results obtained for this case. As seen, the difference in MTOM amounts to 1% and in non-propulsive airframe mass to less than 1%. The simulated aircraft is extremely close to the real one also when looking at other quantities, such as wing surface and power installed. A higher error is observed in the fuel mass, a quantity that is clearly sensitive to the assumed equivalent specific fuel consumption (ESFC) of the turboprop engines.

4.3. Large regional

The third case study involves a much larger aircraft in the CS25 category, the ATR72-600. It is a up to 78-passenger, pressurized, turboprop, high-wing aircraft powered by a pair of Pratt & Whitney Canada PW127M, providing for a cruising speed of 280 kn. This aircraft is one of the most common regional airliners worldwide and may typify the upper end of mid-future HE applications in air transportation.

The Hyperion design solution was obtained by imposing a sizing mission characterized by the official data for this type, including a range of 1,530

km with 70 passengers on board.

Tab. 3 shows some of the results obtained for this case. As seen, the difference in MTOM and in non-propulsive airframe mass are negligible, as those in wing surface and power installed, making the simulated aircraft a copy of the real one.

Table 3. Validation for the ATR72-600 regional aircraft.

| ATR72-600 | M_{mto} [kg] | M_a [kg] | M_f [kg] | S [m ²] | P_b [kW] |
|-----------|----------------|------------|------------|-----------------------|------------|
| Real | 23,000 | 13,500 | 2,000 | 61.0 | 3,650 |
| Simulated | 22,990 | 13,450 | 1,920 | 61.8 | 3,930 |
| Error [%] | 0.0 | 0.0 | -0.4 | 0.0 | +0.1 |

The higher accuracy shown for larger weight types (Beechcraft 1900D and ATR72-600) compared to the Tecnam P2012 is attributed to the much smaller scattering in the operational empty mass fraction data.

4.4. Panthera Hybrid

The Panthera Hybrid is a serial HE aircraft derived by the piston-engine powered Panthera, a CS23 category aircraft designed and manufactured by the Slovenian Pipistrel. The original Panthera is an all-composite, four-seat General Aviation aircraft powered by a Lycoming IO-540, providing for a cruising speed of 200 kn. It has been chosen as the candidate for a high-technology retrofit based on a serial HE powertrain based on a new 200 kW EM and a 110 kW PGS.

The Hyperion design solution was obtained by imposing a sizing mission according to company data.

Table 4. Validation for the Pipistrel Panthera Hybrid aircraft.

| Panthera Hybrid | M_{mto} [kg] | $M_a + M_m + M_g$ [kg] | M_b [kg] | M_f [kg] |
|-----------------|----------------|------------------------|------------|------------|
| Real | 1,315 | 830 | 120 | 53 |
| Simulated | 1,369 | 868 | 121 | 68 |
| Error [%] | 0.0 | 0.0 | 0.0 | +0.3 |

Tab. 4 and Fig. 4 show some of the results obtained for this case. In Fig. 4, top, the complete mass breakdown is shown, with the inner ring corresponding to the real aircraft and the outer to the simulated aircraft. The combination ($M_a + M_m + M_g$) in the table corresponds to the “empty mass” seen in this graph. In Fig. 4, bottom, a comparison is made between the power values obtained for the EM and the PGS (blue: real aircraft; purple: simulated aircraft). The high accuracy of the preliminary sizing through Hyperion is apparent, adding to the promising results obtained for conventionally-powered aircraft.

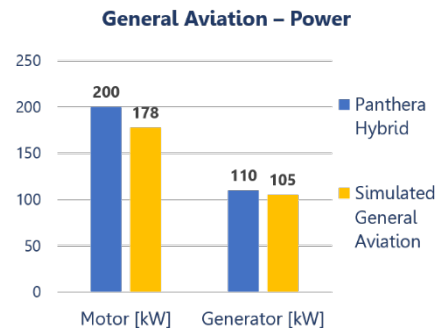
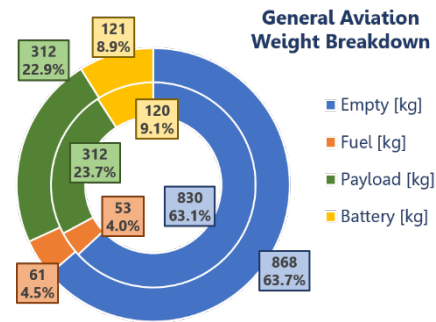


Figure 4. Validation for the Pipistrel Panthera Hybrid aircraft (top: inner ring: Panthera Hybrid; outer ring: simulated aircraft).

5. APPLICATION STUDIES

In order to illustrate the capabilities of the proposed methodology, a few applications are reported in the following.

5.1. General Aviation

First, we are concerned with a small General Aviation (GA) aircraft, inspired by a well-known model, the Cessna 172. This piston-powered, single-engine aircraft is a mainstay in GA worldwide and provides the capability of hosting four occupants for a range of 960 km.

A first serial HE design solution, named A4H, was investigated by considering the same sizing mission specifications of the Cessna 172. Compliance with CS23 requirements, i.e. point and terminal performance (related to sizing to power), as well as fuel reserves for a 45-minute loiter at 1,500 ft (impacting on sizing to energy) was requested.

Fig. 2 shows the SMP for this case, with the chosen design point. The hybrid transition altitude was set to 1,300 ft (~400 m), both in climb and descent. The selected battery technology involves $p_b = 2.200$ kW/kg and $e_b = 0.239$ kWh/kg. This allows the BP to be sized according to power needs (thus, extra energy is available).

The maximum and minimum allowed BP SOC values are set at 85% and 20%, respectively. In addition, end-of-flight stored energy requirements are imposed, calling for minimum BP SOC and 5% fuel remaining at landing. A further prescription is a 50% EM extra power (a value applicable to the Panthera Hybrid).

The value for the A4H MTOM is found as 1,235 kg, which represents a 15% increase compared to the original Cessna 172 value. The corresponding values for installed power and wing reference surface are 121.8 kW and 17.1 m².

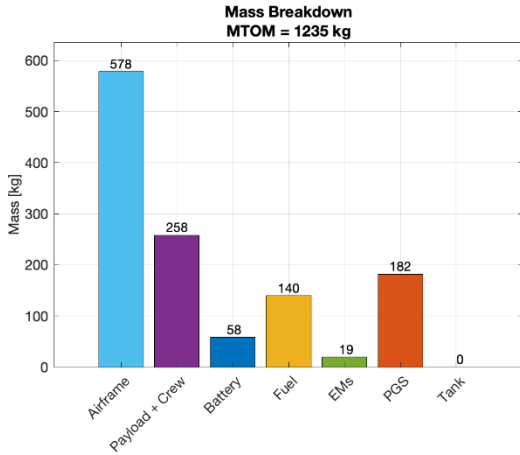


Figure 5. Mass breakdown for the A4H solution.

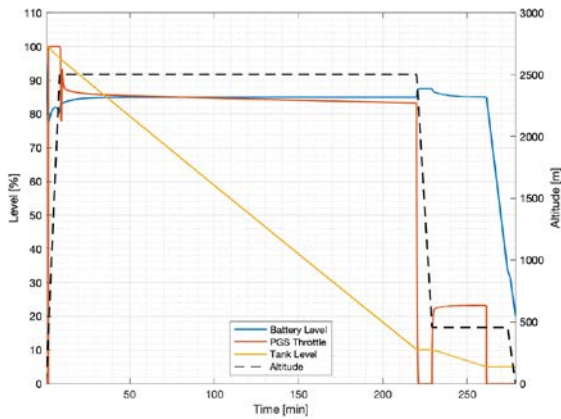


Figure 6. Time histories of battery state of charge (blue), PGS throttle (red), fuel quantity (yellow), and altitude (black) for the A4H.

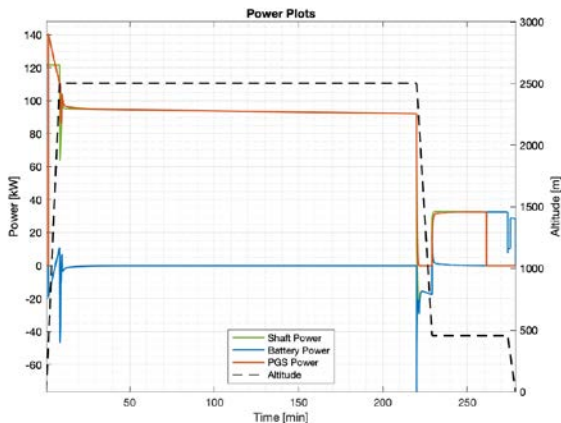


Figure 7. Time histories of shaft power (green), BP power (blue), PGS power (red), and altitude (black) for the A4H.

Fig. 5 shows the mass breakdown for the A4H: it is seen that the non-propulsive airframe mass M_a amounts to 46.8% of M_{mto} , while M_b , M_f , M_m , M_g

represent the 4.7%, 11.3%, 1.5%, 14.7%, respectively. The payload mass ratio is $\frac{M_p}{M_{mto}} = 20.9\%$.

Figs. 6 and 7 depict the time evolution of the energy stored on board, obtained by applying an optimal energy management strategy [4]. In Fig. 6, the BP SOC, fuel quantity, and PGS throttle level are shown, together with the altitude profile, while in Fig. 7, the corresponding values for shaft power, BP power, and PGS power are shown, again together with the altitude profile.

It can be seen that the battery is discharged only during the PE phases (which indeed last only a few minutes), while it is charged throughout the rest of the flight and discharged again towards the end of the loiter and in the final descent. The PGS is kept running during the BP charging phases (without the need to operate at maximum rating) to provide the recharge. Negative values of BP power in Fig. 7 correspond to charging phases. Once the BP SOC is sufficient to carry out the final part of the mission, insuring the required residual energy at flight completion, the PGS is shut down permanently.

A second serial HE solution, named B4H, was sought, by looking at the range allowed by limiting the MTOM to the original Cessna 127 value, i.e. 1,073 kg, and reducing the loiter to 15 minutes. Keeping the same battery technology and all other applicable performance constraints, as well as the same limitations for battery SOC, end-of-flight stored energy, and EM extra power, a maximum range of 400 km was found (41.6% less than the original Cessna 172) for the B4H. The corresponding values for installed power and wing reference surface are 113.5 kW and 14.4 m², or 6.8% and 15.8% lower than the A4H, respectively.

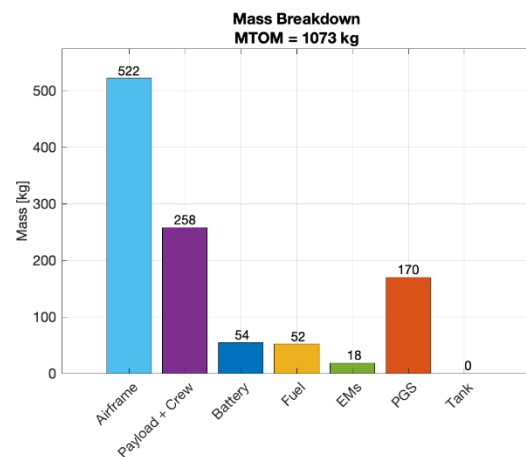


Figure 8. Mass breakdown for the B4H solution.

Fig. 8 shows the mass breakdown for this lighter solution, which requires 88 kg (or 63%) less fuel, while asking for only slightly lower masses for BP, EM and PGS. This is clearly an effect of the sizing to power, which induces only slight changes in all mass components except fuel, even when a

significant change in range is imposed. The payload mass ratio amounts to the original Cessna 172 value, i.e. $\frac{M_p}{M_{mto}} = 24.0\%$.

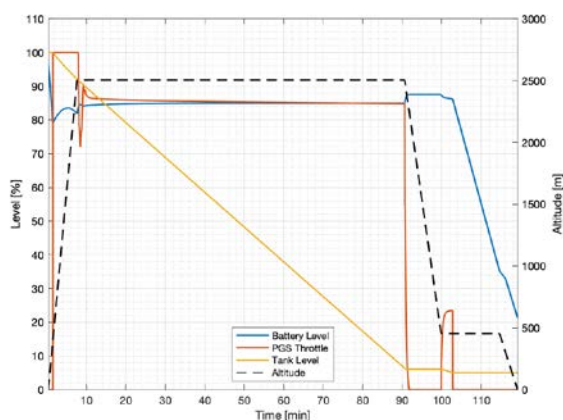


Figure 9. Time histories of battery state of charge (blue), PGS throttle (red), fuel quantity (yellow), and altitude (black) for the B4H.

The time evolution of the energy stored on board is shown in Fig. 9, depicting BP SOC, fuel quantity, and PGS throttle level, together with the altitude profile. It is noted that the only significant difference with the A4H case lies in the shorter activation of the PGS during loiter, as a result of the abundant energy stored in the BP. This allows to fly most of the loiter in PE mode, even if above the hybrid transition altitude.

A third variant, this time a PE one was considered. This, named B4A, was sized by keeping the same range and loiter provisions as the B4H, as well as all other applicable performance constraints. In this case, since a PE solution is better sized according to energy, different battery cells have been adopted, with a lower specific power value, $p_b = 1.500$ kW/kg, and a higher specific energy value, $e_b = 0.483$ kWh/kg. The same limitations for battery SOC and end-of-flight battery stored energy, as well as EM extra power are applied.

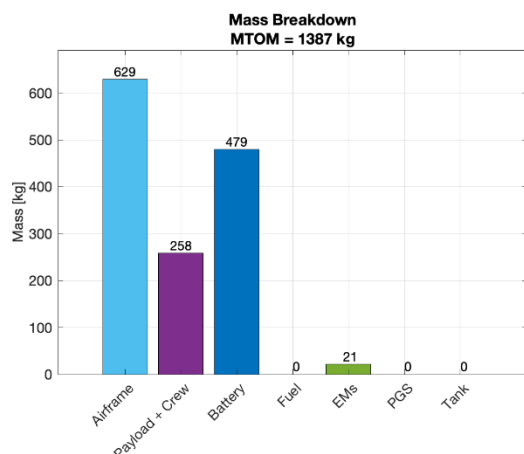


Figure 10. Mass breakdown for the B4A solution.

The value for the B4A MTOM is found as 1,387 kg,

which represents a 29% increase compared to the original Cessna 172 value. The corresponding values for installed power and wing reference surface are 134.4 kW and 19.3 m², or 18.4% and 34.0% higher than the B4H, respectively.

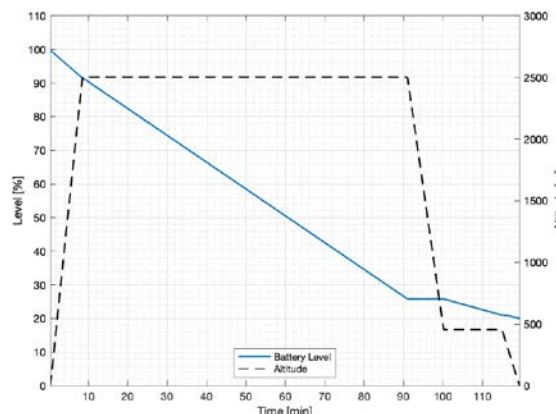


Figure 11. Time histories of battery state of charge (blue) and altitude (black) for the B4A.

Fig. 10 shows the mass breakdown for the B4A: it is seen that the non-propulsive airframe mass M_a amounts to 45.3% of M_{mto} , while M_b and M_m represent the 34.5% and 1.5%, respectively. The payload mass ratio is $\frac{M_p}{M_{mto}} = 18.6\%$.

For completeness, Fig. 11 shows the time evolution of the energy stored on board, contrasting the BP SOC with the altitude profile.

5.2. Commuter

Another case study concerns a 19-passenger commuter. In this case, a HE solution has been retrieved by applying the mission requirements of the Dornier Do 228, a twin-turboprop, STOL utility aircraft certified in the CS23 commuter category. This aircraft provides a range of 400 km with 19 passengers on board, with provisions for a 35-minute loiter.

The HE design solution, named A19H, has been sought by imposing similar technology and mission profile parameters as those seen for the A4H. In particular, the same battery performance and SOC limits, end-of-flight stored energy, and hybrid transition altitude are applied. The EM overrating has been lowered to 25%, in view of the larger size of the motors and the consequent higher cooling burden.

The value for the A19H MTOM is found as 8,991 kg, which is 3.2% higher than the current CS23 design mass limit of 8,618 kg. The corresponding values for total installed power and wing reference surface are 1,922 kW and 44.9 m².

Fig. 12 shows the mass breakdown for the A19H: it is seen that the non-propulsive airframe mass M_a amounts to 54.1% of M_{mto} , while M_b , M_f , M_m , M_g represent the 8.3%, 5.8%, 2.7%, 5.9%, respectively. The payload mass ratio is $\frac{M_p}{M_{mto}} =$

24.4%. These numbers greatly differ from those seen in the A4H and B4H cases, hinting to the difficulty to scale results from one weight category to another, and to the need to employ refined estimation methods to obtain reliable information, albeit at a preliminary sizing level.

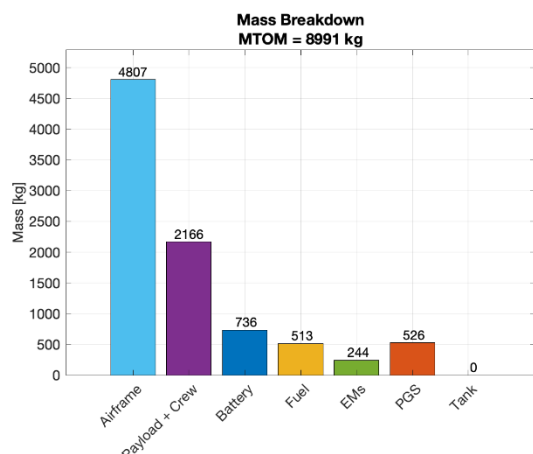


Figure 12. Mass breakdown for the A19H solution.

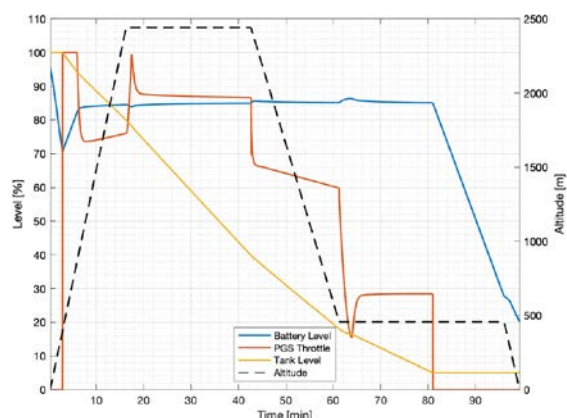


Figure 13. Time histories of battery state of charge (blue), PGS throttle (red), fuel quantity (yellow), and altitude (black) for the A19H.

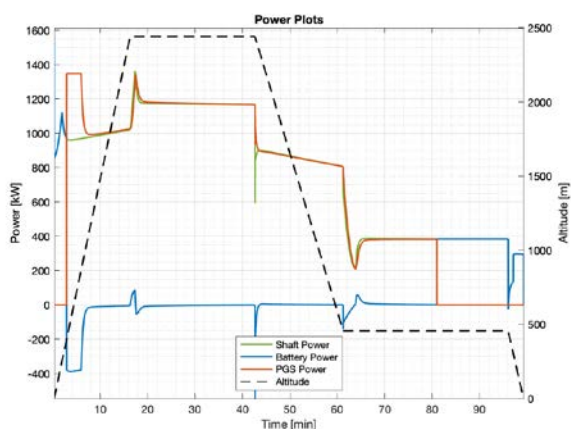


Figure 14. Time histories of shaft power (green), BP power (blue), PGS power (red), and altitude (black) for the A19H.

Figs. 13 and 14 depict the time evolution of the energy stored on board, again obtained through an optimal energy management. It is readily seen that,

while BP SOC globally follows a similar trend as in the A4H and B4H cases, the PGS is invoked at different throttle levels during the sizing mission. Apart from small-duration boosts, BP recharge only occurs significantly after crossing the hybrid transition altitude in climb, ending well before reaching the top of climb. In this case, the loiter is performed half in HE mode and half in PE mode.

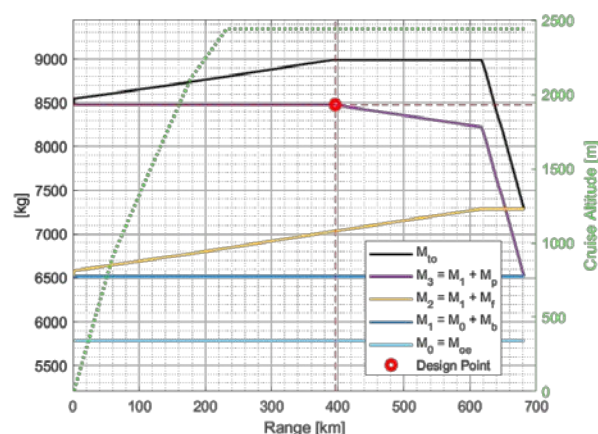


Figure 15. Evolution of mass components as a function of off-design range for the A19H.

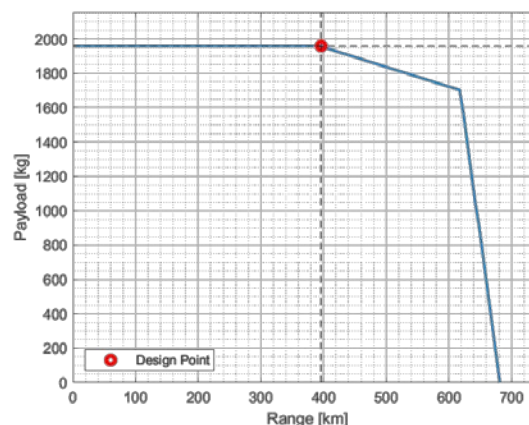


Figure 16. Payload-range diagram for the A19H.

Off-design performance is highly relevant, especially for transport aircraft. Therefore a payload-range analysis for the A19H was performed. Fig. 15 shows the dependence of mass components on off-design range. The black line shows the take-off mass (TOM) according to the three typical operating modes: below design range, TOM increases as fuel is added at full payload, until reaching the MTOM value; from there on, payload is traded off with fuel, in order to achieve higher ranges, up to tank complete filling; finally, ferry range, i.e. the maximum distance flyable at null payload, is achieved, by progressively decreasing payload. From this, the payload-range diagram in Fig. 16 is obtained.

6. CONCLUSION

The present paper introduces a novel methodology aiming to perform the preliminary sizing of innovative, electrically-powered fixed-wing aircraft, providing a comprehensive and flexible tool for conceptual/preliminary design loops. The methodology can deal with pure-electric (battery-based) airplanes, as well as serial hybrid-electric ones, and is currently being extended to fuel-cell driven airplanes as well.

A validation effort including several conventional aircraft across widely different weight categories, from low-end CS23 to CS25 models, has been carried out, together with some similar studies involving pure-electric and hybrid-electric aircraft. Examples of these studies have been detailed here.

Based on this methodology, a number of design exercises have been pursued. The present discussion, involving a 4-seat and a 19-passenger airplane in multiple versions, provides an illustration of the flexibility and power in tackling widely different design cases, in view of fully-fledged design exercises as those foreseen in the MAHEPA and UNIFIER19 projects.

A further application of the presented methodology is found in a companion paper [10].

7. FUNDING

This research was partially funded by the EU Horizon 2020 research and innovation program, under project MAHEPA, GA N. 723368.

8. REFERENCES

1. Trainelli, L., & Perkon, I. (2019). MAHEPA – A Milestone-Setting Project in Hybrid-Electric Aircraft Technology Development. In Proc. More Electric Aircraft Conference (MEA 2019), Toulouse, France.
2. Riboldi, C., Gualdoni, F. (2016). An Integrated Approach to the Preliminary Weight Sizing of Small Electric Aircraft. *Aerospace Science and Technology* **58**, 134–149.
3. Riboldi, C. E. D., Gualdoni, F., & Trainelli, L. (2018). Preliminary Weight Sizing of Light Pure-Electric and Hybrid-Electric Aircraft. *Transportation Research Procedia* **29**, 376–389.
4. Trainelli, L., Riboldi, C. E. D., Salucci, F., & Rolando, A. (2019). Preliminary Sizing and Energy Management of Serial Hybrid-Electric Airplanes. In Proc. XXV AIDAA Congress, Roma, Italy.
5. Roskam, J. (2003). *Airplane Design: Parts I through VIII*. Roskam Aviation and Engineering Corporation.
6. Raymer, D. (2012). *Aircraft Design: A Conceptual Approach*. American Institute of Aeronautics and Astronautics, Inc..
7. Brelje, B. J. & Martins, J. R. R. A. (2018). Electric, hybrid, and turboelectric fixed-wing aircraft: A review of concepts, models, and design approaches. *Progress in Aerospace Sciences* **104**, 1-19.
8. Trainelli, L., Salucci, F., Comincini, D., Riboldi, C. E. D. & Rolando, A. (2019). Sizing and Performance of Hydrogen-Driven Airplanes. In Proc. XXV AIDAA Congress, Roma, Italy.
9. Riboldi, C. E. D., Mariani, L., Trainelli, L., Rolando, A. & Salucci, F. (2020). Assessing the Effect of Hybrid-Electric Power-Trains on Chemical and Acoustic Pollution. In Proc. Aerospace Europe Conference (AEC 2020), Bordeaux, France.
10. Arditi, M., D'Ascenzo, A., Montorfano, G., Poiana, G., Rossi, N., Sesso, M., Spada, C., Riboldi, C.E.D. & Trainelli L. (2018). An Investigation of the Micro-Feeder Aircraft Concept. In Proc. Advanced Aircraft Efficiency in a Global Air Transport System Conference (AEGATS 2018), Toulouse, France.
11. Rolando, A., Salucci, F., Trainelli, L., Riboldi, C. E. D. (2020). On the Design of an Electric-Powered Micro-Feeder Aircraft. In Proc. Aerospace Europe Conference (AEC 2020), Bordeaux, France.
12. Bruglieri, M., Marchionni, A. M. & Trainelli, L. (2019). Optimization of the Demand Satisfied by a 'Micro-Feeder' Hybrid-Electric Air Transport Service. In Proc. XXV Congresso Nazionale AIDAA, Roma, Italy.
13. Trainelli, L., Bruglieri, M., Salucci, F. & Gabrielli, D. (2020). Optimal Definition of a Short-Haul Air Transportation Network for Door-to-Door Mobility. In Proc. Aerospace Europe Conference (AEC 2020), Bordeaux, France.